PNAS RESEARCH ARTICLE | NEUROSCIENCE OPEN ACCESS

Evidence of association between higher cardiorespiratory fitness and higher cerebral myelination in aging

Mary E. Faulkner[a,1], Zhaoyuan Gong[a,1], Murat Bilgel[b], John P. Laporte[a], Alex Guo[a], Jonghyun Bae[a], Elango Palchamy[c], Mary Kaileh[d], Christopher M. Bergeron[a], Jan Bergeron[a], Sarah Church[d], Jarod D'Agostino[d], Luigi Ferrucci[c], and Mustapha Bouhrara[a,2]

Affiliations are included on p. 7.

Edited by Joseph Takahashi, The University of Texas Southwestern Medical Center, Dallas, TX; received February 13, 2024; accepted July 10, 2024

Emerging evidence suggests that altered myelination is an important pathophysiologic correlate of several neurodegenerative diseases, including Alzheimer and Parkinson's diseases. Thus, improving myelin integrity may be an effective intervention to prevent and treat age-associated neurodegenerative pathologies. It has been suggested that cardiorespiratory fitness (CRF) may preserve and enhance cerebral myelination throughout the adult lifespan, but this hypothesis has not been fully tested. Among cognitively normal participants from two well-characterized studies spanning a wide age range, we assessed CRF operationalized as the maximum rate of oxygen consumption (VO_2max) and myelin content defined by myelin water fraction (MWF) estimated through our advanced multicomponent relaxometry MRI method. We found significant positive correlations between VO_2max and MWF across several white matter regions. Interestingly, the effect size of this association was higher in brain regions susceptible to early degeneration, including the frontal lobes and major white matter fiber tracts. Further, the interaction between age and VO_2max exhibited i) a steeper positive slope in the older age group, suggesting that the association of VO_2max with MWF is stronger at middle and older ages and ii) a steeper negative slope in the lower VO_2max group, indicating that lower VO_2max levels are associated with lower myelination with increasing age. Finally, the nonlinear pattern of myelin maturation and decline is VO_2max-dependent with the higher VO_2max group reaching the MWF peak at later ages. This study provides evidence of an interconnection between CRF and cerebral myelination and suggests therapeutic strategies for promoting brain health and attenuating white matter degeneration.

myelin | cardiorespiratory fitness | MRI | aging

Significance

Research suggests that maintaining good cardiorespiratory fitness (CRF) plays a role in preserving white matter integrity. However, there is scarcity of clinical studies examining the relationship between CRF and myelin integrity. Here, we investigated the association between CRF, as measured by the maximum rate of oxygen consumption (VO_2max), and myelin content, as defined by the myelin water fraction (MWF) MRI, throughout the adult lifespan. Higher VO_2max is associated with greater cerebral myelination, particularly in middle-aged and older adults, providing insights into the potential protective role of CRF in attenuating demyelination in aging. While our study does not establish causality, it highlights the importance of CRF in maintaining white matter health and warrants further investigation into the underlying mechanisms influencing myelination.

White matter abnormalities are associated with higher risks of cognitive decline and future development of neurodegenerative diseases, with evidence suggesting a causal link to Alzheimer's disease (AD) (1, 2). Degradation of myelin sheaths, the protective lipid layer produced and maintained by oligodendrocytes, is now considered a primary and proximal cause of white matter damage, revealed by white matter hyperintensities often observed in structural neuroimaging (3). Although growing evidence suggests that lifestyle factors, such as physical activity, can offset the degradation of white matter structure and function (4), clinical in vivo investigations of the specific relationship between myelin integrity and modifiable lifestyle factors are lacking. Yet, such studies are sine qua non for advancing our understanding of brain aging, which could lead to promising and relevant avenues for the development of tailored interventions to promote brain health, to mitigate brain demyelination, and to potentially delay the onset or progression of age-related neurodegenerative diseases.

It has been suggested that the maintenance of good cardiorespiratory fitness (CRF) may help to prevent or slow down age-associated degeneration of cerebral tissue integrity. CRF refers to the capacity of an individual's cardiovascular and respiratory systems to deliver oxygen to skeletal muscles during sustained moderate- to high-intensity physical activity (5). As a modifiable lifestyle factor, CRF can be enhanced through various aerobic fitness activities including walking, running, swimming, and biking (6). The results of previous human neuroimaging studies suggest that higher CRF is associated with conserved brain structure and function (5, 7), improved cognitive function and slowing of cognitive decline (8), and delayed progression of neurodegenerative diseases, including AD (9). In this context, there has been growing attention to the relationship between CRF and white matter macro- and microstructural integrity. Studies utilizing structural MRI and diffusion tensor imaging (DTI) have reported associations between higher CRF and greater white matter volumes (10, 11), fewer white matter lesions (12, 13), and greater white matter microstructural integrity, as typically indicated by higher fractional anisotropy and lower mean and radial diffusivities (6, 14, 15). Similar findings have also been reported

The authors declare no competing interest.

This article is a PNAS Direct Submission.

[1]M.E.F. and Z.G. contributed equally to this work.

[2]To whom correspondence may be addressed. Email: bouhraram@mail.nih.gov.

This article contains supporting information online at https://www.pnas.org/lookup/suppl/doi:10.1073/pnas.2402813121/-/DCSupplemental.

Published August 19, 2024.

in the context of several neurodegenerative diseases, including mild cognitive impairment, AD, and multiple sclerosis (16–18).

However, previous investigations were mostly based on conventional structural MRI and DTI techniques, which are not specific to any determinant of white matter tissue. Indeed, although sensitive to changes in brain tissue demyelination, the underlying structural mechanisms responsible for these derived indices are difficult to define due to their sensitivity to other intrinsic methodological and physiological factors, such as macromolecular content, axonal degeneration, and architectural features including fiber fanning and crossing. Furthermore, the DTI indices represent a weighted average of all water compartments, losing their specificity as markers for a particular tissue. Advanced quantitative MRI methods based on multicomponent relaxometry have since been introduced that are more sensitive and specific for measuring myelin content in vivo (19). In particular, the Bayesian Monte Carlo multicomponent driven equilibrium single pulse observation of T_1 and T_2 (BMC-mcDESPOT) analysis enables robust quantification of whole-brain (WB) and local myelin water fraction (MWF), a direct and specific proxy of myelin content (20–22). Notably, this methodology has been utilized in recent investigations reporting positive associations between MWF and cerebral blood flow (23, 24) and motor function (25), both of which are known to be influenced by CRF, thereby adding further motivation to our primary hypothesis of an association between higher CRF and higher MWF.

While previous work explored the relationships between factors affecting cardiovascular fitness, including hypertension (26), cerebral blood flow, and obesity (23, 27), the specific relationship between white matter health, reflected by MWF, and the maximum rate of oxygen consumption (VO_2max), a comprehensive measure of cardiovascular fitness influenced by multiple interrelated risk factors, has not been established. Here, we investigated the association between CRF and regional myelin content in a large cohort of cognitively unimpaired adults (N = 144), spanning an extended age range of 22 to 94 y. Myelin content was assessed using our BMC-mcDESPOT-MWF method, while CRF was assessed by VO_2max, as per our established fitness protocol. VO_2max is ubiquitously used as the gold standard measure of CRF and a hallmark biomarker of health and longevity in both laboratory and clinical settings. It reflects an individual's maximum physiological capacity to take in, transport, and use oxygen during strenuous physical activity. Through this investigation, we aim to gain further insights into the underlying mechanisms by which CRF promotes brain health and attenuates white matter demyelination in aging.

Results

Cohort's Characteristics. Participant characteristics are shown in Table 1. After excluding nine participants due to cognitive impairments, four due to missing VO_2max data, and six datasets due to low image quality, mainly because of severe motion artifacts, the final study cohort consisted of 125 cognitively unimpaired participants, ranging in age from 22 to 94 y (56.3 ± 20.8 y). Sixty-eight participants (54.4%) were men. Mean ± SD of systolic blood pressure (SBP) and VO_2max were 117.4 ± 14.4 mmHg and 27.9 ± 8.2 mL/kg/min, respectively. However, our cohort was dominantly composed of White participants (71.2%).

Associations between CRF and Cerebral Myelination. Fig. 1 displays axial and sagittal MWF parameter maps averaged across participants with either low, moderate, or high VO_2max values within restricted age ranges of 22 to 39 y, 40 to 59 y, 60 to 79 y, and 80 to 94 y. Results derived from the entire cohort (22 to 94 y) are also shown. These restricted age ranges were used to minimize the potential effect of age on derived MWF parameter maps for this qualitative analysis. The total number of participants for each group is also reported. The statistical quantification of the effect of age as a covariate is presented in Table 2. Lower VO_2max corresponds to values below the 30th percentile value, moderate VO_2max corresponds to values between the 30th and 70th percentile values, and higher VO_2max corresponds to values equal to or above the 70th percentile value. We examined whether mean ages differed between any pair of VO_2max groups within each age bin by using two sample t tests. We found statistically significant differences within the full age range bin (22 to 94 y) and in the highest age bin (80 to 94 y) when comparing the moderate VO_2max group to the other two VO_2max groups, with a slightly higher mean age for the moderate VO_2max group (less than 4 y). We did not observe statistically significant VO_2max group differences within the remaining age bins. Visual inspection indicates that, overall, participants with lower VO_2max values exhibit lower regional MWF values, and, conversely, participants with higher VO_2max values exhibit higher regional MWF values, especially in middle and older age ranges. Therefore, higher CRF seems to be associated with higher cerebral myelin content, thereby suggesting a potential direct association between VO_2max and myelination. Similar results are readily seen in *SI Appendix*, Fig. S1 providing results with additional and more restricted age ranges/bins of 22 to 39 y, 40 to 52 y, 53 to 69 y, 70 to 79 y, and 80 to 94 y, but stratified into lower (VO_2max ≤ 50th percentile) or higher (VO_2max > 50th percentile) groups to ensure a sufficient number of subjects per group. Here, as well, besides the VO_2max groups of the full age range (22 to 94 y), all mean ages between groups were found to be not statistically significant after the two-sample t test.

Fig. 2 shows plots of the associations between MWF and VO_2max or age, derived from the WB white matter, from the two linear regression models, with model #1 adjusting for age, sex, and SBP while model #2 adjusting for age, age^2, sex, and SBP. Results derived from the remaining ROIs are shown in *SI Appendix*, Figs. S1–S5. In agreement with the visual inspection (Fig. 1), there is a positive correlation between VO_2max and MWF, with higher VO_2max values corresponding to higher MWF values (Fig. 2 *I* and *V*). This association was stronger and more significant for model #2. However, it is readily seen from the age-stratified associations between MWF and VO_2max derived from model #1 (Fig. 2*III*) and model #2 (Fig. 2*VII*) that,

Table 1. Demographic characteristics of study participants

Total sample	N = 125
Age (y), mean ± SD (min-max)	56.3 ± 20.8 (22–94)
Sex	
Male, N (%)	68 (54.4%)
Female, N (%)	57 (45.6%)
Race	
White, N (%)	89 (71.2%)
Black, N (%)	23 (18.4%)
AAPI or Other, N (%)	13 (10.4%)
SBP (mmHg), mean ± SD (min-max)	117.4 ± 14.4 (89–161)
VO_2max (mL/kg/min), mean ± SD (min-max)	27.9 ± 8.2 (9.6–49.7)

Notes. SBP, systolic blood pressure; VO_2max, maximum volume rate of oxygen; SD, Standard deviation; min, minimum; max, maximum; AAPI, Asian American and Pacific Islander. Values are given as either the mean ± SD (range), or the N(%).

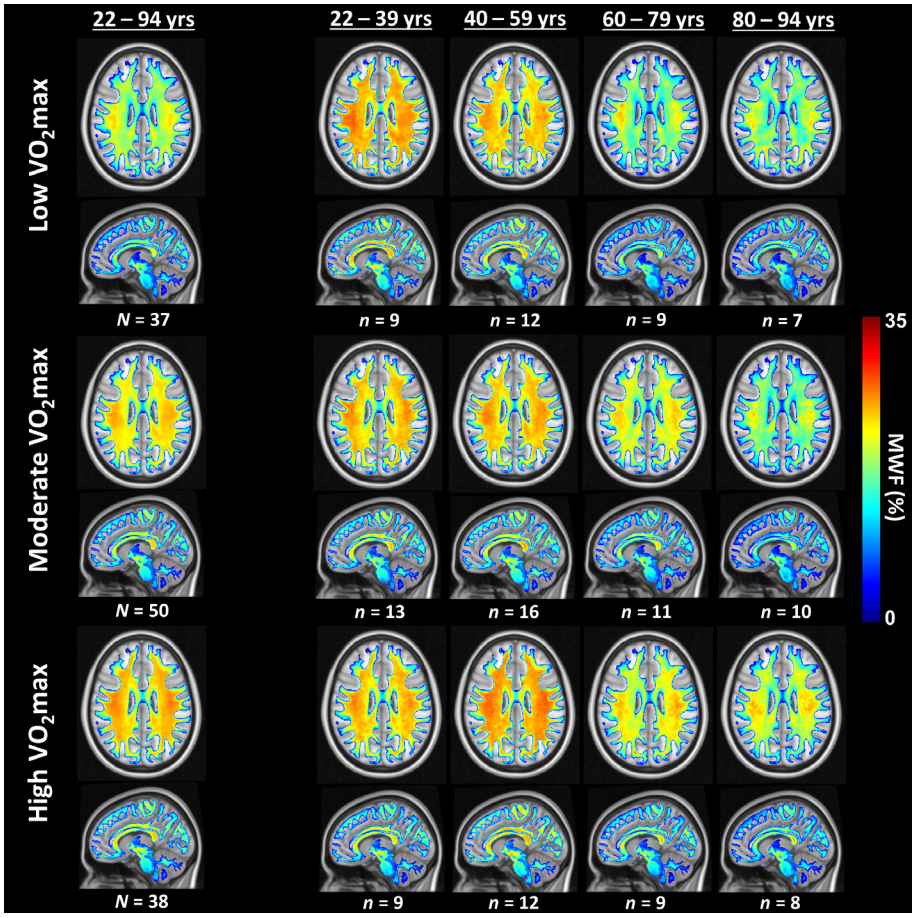

Fig. 1. Examples of axial and sagittal MWF parameter maps averaged across participants with either lower, moderate, or higher VO_2max levels. Participants were drawn from the full age range as well as from restricted age ranges to mitigate the effect of age. Results are shown for representative slices. Visual inspection indicates that, overall, participants with higher VO_2max levels exhibit greater regional MWF values, especially at middle and older ages.

while this association is positive for all age groups, the older age group exhibits the steepest slope followed by the middle age group, suggesting that the effect of VO_2max on MWF is strongest at middle and older ages. Moreover, Figs. 2 *II* and *VI* show the association between MWF and age derived from model #1 and model #2, respectively. While a negative association between age and MWF was observed using model #1 (Fig. 2*II*), model #2 shows a nonlinear association between age and MWF, with increased MWF values until middle age followed by a decline afterward (Fig. 2*VI*). The year of maximum myelination (i.e., peak MWF) was observed around 31 y of age for WB white matter. Here again, this association was VO_2max-dependent (Fig. 2*IV* and *VIII*). Specifically, using model #1, a steeper negative slope in the lower VO_2max group was observed followed by the middle age group, indicating that lower VO_2max levels are associated with more rapid demyelination with advanced ages (Fig. 2*IV*). Using model #2, results show that the nonlinear pattern of myelin maturation and decline is VO_2max-dependent with the higher VO_2max group reaching the MWF peak at later ages (around ~41 y), as compared the other groups (Fig. 2*VIII*), with the moderate VO_2max group reaching the MWF peak at around 27.8 y while the MWF peak for the low VO_2max group was outside the age range of this cohort. This result indicates that the myelin maturation process is hampered with a poorer CRF while leading to a decline in myelination starting at younger ages. Similar observations are seen in most ROIs, with results displayed in *SI Appendix*, Figs. S1–S5. Of note, while the lower VO_2max group appears to have slightly higher MWF values compared to the moderate and higher VO_2max subgroups at younger ages (Fig. 1), differences in MWF values between these groups in this age range are not statistically significant, as shown by the overlapping CI in Fig. 2*IV*.

Table 2 summarizes the results of the multiple linear regression models for all 14 white matter ROIs investigated. We note that, for sake of clarity and simplicity, only the relevant regression terms, namely, age, age^2, VO_2max, and interactions are shown. The full results including the remaining covariates are shown in *SI Appendix*, Table S1. First, using model #1, results indicate that the association between VO_2max and MWF was positive and significant in all ROIs, except OL, PL, TL, CRB, and CC, even after FDR correction. The effect size of this association was stronger and significant in all ROIs using model #2, including in the anterior brain regions such as the FL and TL as well as in the white matter tracts including CR, TL, LF, FOF, and FOR as compared to the posterior brain regions such as the OL, PL, and CRB. This association was age-dependent as reflected by the age×-VO_2max (model #1) or age^2 × VO_2max (model #2) interaction terms, exhibiting significant associations with MWF in all ROIs before and after FDR correction, except for CRB using model #1. Finally, for both regression models, age exhibited negative association with MWF which was significant in all ROIs except for CP. Here again, this association was stronger using model #2. However, using model #2, the association between age^2 and MWF was found to be significant ($P < 0.05$) or close to significance ($P < 0.1$) in a few ROIs, namely, WB, FL, LF, CC, IC, and FOR, but did not survive FDR correction.

Table 2. Regression coefficient (SE) and *P*-values [before, *P*, and after false discovery rate (FDR) correction, P_{FDR}] of age, VO_2max, and age × VO_2max with respect to MWF (Model 1) and age, age^2, VO_2max, age × VO_2max, and age^2 × VO_2max with respect to MWF (Model 2) for each of the 14 WM regions-of-interest (ROIs) investigated.

	MWF							
	Model 1			Model 2				
ROIs	Age	VO_2max	Age × VO_2max	Age	Age^2	VO_2max	Age × VO_2max	Age^2 × VO_2max
WB	−0.37*(0.11)*, **P < 0.001***, **P_{FDR} = 0.003**	0.25*(0.11)*, **P = 0.027**, **P_{FDR} = 0.047**	0.30*(0.09)*, **P < 0.001***, **P_{FDR} = 0.002**	−0.56*(0.12)*, **P < 0.001***, **P_{FDR} < 0.001**	−0.22*(0.12)*, P = 0.061, P_{FDR} = 0.170	0.48*(0.13)*, **P < 0.001***, **P_{FDR} = 0.002**	0.10*(0.11)*, P = 0.359, P_{FDR} = 0.547	−0.31*(0.10)*, **P = 0.002***, **P_{FDR} = 0.005**
FL	−0.40*(0.10)*, P < **0.001***, **P_{FDR} = 0.002**	0.30*(0.10)*, **P = 0.004***, **P_{FDR} = 0.020**	0.31*(0.08)*, **P < 0.001***, **P_{FDR} = 0.001**	−0.58*(0.11)*, **P < 0.001***, **P_{FDR} < 0.001**	−0.21*(0.11)*, **P = 0.049**, P_{FDR} = 0.170	0.51*(0.13)*, **P < 0.001***, **P_{FDR} = 0.001**	0.13*(0.11)*, P = 0.235, P_{FDR} = 0.547	−0.28*(0.09)*, **P = 0.002***, **P_{FDR} = 0.005**
OL	−0.26*(0.12)*, **P = 0.038**, **P_{FDR} = 0.044**	0.15*(0.13)*, P = 0.219, P_{FDR} = 0.236	0.31*(0.09)*, **P = 0.002***, **P_{FDR} = 0.003**	−0.47*(0.14)*, **P <0.001***, **P_{FDR} < 0.001**	−0.26*(0.12)*, **P = 0.049**, P_{FDR} = 0.170	0.41*(0.16)*, **P = 0.010**, **P_{FDR} = 0.011**	0.08*(0.13)*, P = 0.546, P_{FDR} = 0.588	−0.35*(0.11)*, **P = 0.002***, **P_{FDR} = 0.005**
PL	−0.39*(0.11)*, P < **0.001***, **P_{FDR} = 0.003**	0.18*(0.11)*, P = 0.111, P_{FDR} = 0.141	0.29*(0.08)*, **P = 0.001***, **P_{FDR} = 0.003**	−0.55*(0.12)*, **P < 0.001***, **P_{FDR} < 0.001**	−0.15*(0.12)*, P = 0.230, P_{FDR} = 0.268	0.37*(0.14)*, **P = 0.011**, **P_{FDR} = 0.011**	0.15*(0.12)*, P = 0.202, P_{FDR} = 0.547	−0.25*(0.10)*, **P = 0.015**, **P_{FDR} = 0.018**
TL	−0.35*(0.12)*, **P = 0.004***, **P_{FDR} = 0.005**	0.18*(0.12)*, P = 0.136, P_{FDR} = 0.158	0.26*(0.09)*, **P = 0.006**, **P_{FDR} = 0.007**	−0.55*(0.13)*, **P <0.001***, **P_{FDR} < 0.001**	−0.24*(0.13)*, P = 0.057, P_{FDR} = 0.170	0.42*(0.15)*, **P = 0.006**, **P_{FDR} = 0.008**	0.05*(0.12)*, P = 0.706, P_{FDR} = 0.706	−0.33*(0.11)*, **P = 0.003***, **P_{FDR} = 0.005**
CRB	−0.25*(0.13)*, P = 0.059, P_{FDR} = 0.063	0.15*(0.13)*, P = 0.265, P_{FDR} = 0.265	0.10*(0.10)*, P = 0.326, P_{FDR} = 0.326	−0.46*(0.14)*, **P = 0.002***, **P_{FDR} = 0.002**	−0.21*(0.14)*, P = 0.126, P_{FDR} = 0.197	0.41*(0.17)*, **P = 0.015**, **P_{FDR} = 0.015**	−0.10*(0.14)*, P = 0.461, P_{FDR} = 0.547	−0.34*(0.12)*, **P = 0.004***, **P_{FDR} = 0.006**
CC	−0.41*(0.11)*, **P < 0.001***, **P_{FDR} = 0.002**	0.22*(0.11)*, **P = 0.046**, P_{FDR} = 0.064	0.30*(0.09)*, **P < 0.001***, **P_{FDR} = 0.002**	−0.54*(0.12)*, **P < 0.001***, **P_{FDR} < 0.001**	−0.19*(0.12)*, P = 0.095, P_{FDR} = 0.184	0.36*(0.14)*, **P = 0.011**, **P_{FDR} = 0.011**	0.14*(0.11)*, P = 0.226, P_{FDR} = 0.547	−0.21*(0.10)*, **P = 0.040**, **P_{FDR} = 0.043**
IC	−0.35*(0.11)*, **P = 0.002***, **P_{FDR} = 0.004**	0.27*(0.11)*, **P = 0.018**, **P_{FDR} = 0.038**	0.28*(0.09)*, **P = 0.002***, **P_{FDR} = 0.003**	−0.54*(0.12)*, **P < 0.001***, **P_{FDR} < 0.001**	−0.19*(0.12)*, P = 0.098, P_{FDR} = 0.184	0.51*(0.14)*, **P < 0.001***, **P_{FDR} = 0.001**	0.10*(0.11)*, P = 0.396, P_{FDR} = 0.547	−0.32*(0.10)*, **P = 0.002***, **P_{FDR} = 0.005**
CP	−0.02*(0.13)*, P = 0.876, P_{FDR} = 0.876	0.30*(0.13)*, **P = 0.019**, **P_{FDR} = 0.038**	0.26*(0.10)*, **P = 0.010**, **P_{FDR} = 0.011**	−0.16*(0.14)*, P = 0.254, P_{FDR} = 0.254	−0.15*(0.14)*, P = 0.285, P_{FDR} = 0.285	0.48*(0.16)*, **P = 0.004***, **P_{FDR} = 0.006**	0.12*(0.13)*, P = 0.362, P_{FDR} = 0.547	−0.24*(0.12)*, **P = 0.045**, **P_{FDR} = 0.045**
CR	−0.35*(0.11)*, **P = 0.001***, **P_{FDR} = 0.003**	0.32*(0.11)*, **P = 0.003***, **P_{FDR} = 0.020**	0.32*(0.08)*, **P < 0.001***, **P_{FDR} = 0.001**	−0.50*(0.12)*, **P < 0.001***, **P_{FDR} < 0.001**	−0.13*(0.11)*, P = 0.273, P_{FDR} = 0.285	0.51*(0.14)*, **P < 0.001***, **P_{FDR} = 0.001**	0.19*(0.11)*, P = 0.088, P_{FDR} = 0.547	−0.24*(0.10)*, **P = 0.013**, **P_{FDR} = 0.017**
TR	−0.36*(0.11)*, **P = 0.001***, **P_{FDR} = 0.003**	0.27*(0.11)*, **P = 0.017**, **P_{FDR} = 0.038**	0.26*(0.09)*, **P = 0.004***, **P_{FDR} = 0.005**	−0.55*(0.12)*, **P < 0.001***, **P_{FDR} < 0.001**	−0.17*(0.12)*, P = 0.147, P_{FDR} = 0.206	0.50*(0.14)*, **P < 0.001***, **P_{FDR} = 0.001**	0.09*(0.11)*, P = 0.441, P_{FDR} = 0.547	−0.30*(0.10)*, **P = 0.003***, **P_{FDR} = 0.005**
FOF	−0.33*(0.11)*, **P = 0.003***, **P_{FDR} = 0.004**	0.34*(0.11)*, **P = 0.002***, **P_{FDR} = 0.020**	0.32*(0.09)*, **P < 0.001***, **P_{FDR} = 0.001**	−0.51*(0.12)*, **P < 0.001***, **P_{FDR} < 0.001**	−0.14*(0.11)*, P = 0.230, P_{FDR} = 0.268	0.58*(0.14)*, **P < 0.001***, **P_{FDR} < 0.001**	0.17*(0.11)*, P = 0.126, P_{FDR} = 0.547	−0.30*(0.10)*, **P = 0.002***, **P_{FDR} = 0.005**
LF	−0.35*(0.11)*, **P = 0.003***, **P_{FDR} = 0.004**	0.25*(0.12)*, **P = 0.032**, P_{FDR} = 0.050	0.28*(0.09)*, **P = 0.003***, **P_{FDR} = 0.004**	−0.55*(0.13)*, **P < 0.001***, **P_{FDR} < 0.001**	−0.20*(0.12)*, P = 0.097, P_{FDR} = 0.184	0.49*(0.14)*, **P < 0.001***, **P_{FDR} = 0.002**	0.09*(0.12)*, P = 0.469, P_{FDR} = 0.547	−0.32*(0.10)*, **P = 0.002***, **P_{FDR} = 0.005**
FOR	−0.37*(0.11)*, **P < 0.001***, **P_{FDR} = 0.003**	0.27*(0.11)*, **P = 0.015**, **P_{FDR} = 0.038**	0.29*(0.09)*, **P = 0.001***, **P_{FDR} = 0.002**	−0.54*(0.12)*, **P < 0.001***, **P_{FDR} < 0.001**	−0.25*(0.12)*, **P = 0.034**, P_{FDR} = 0.170	0.46*(0.14)*, **P = 0.001***, **P_{FDR} = 0.002**	0.08*(0.11)*, P = 0.466, P_{FDR} = 0.547	−0.27*(0.10)*, **P = 0.006**, **P_{FDR} = 0.008**

Notes. VO_2max, maximum volume rate of oxygen; MWF, myelin water fraction; WM, white matter; ROI, region-of-interest; WB, whole-brain; FL, frontal lobe; OL, occipital lobe; PL, parietal lobe; TL, temporal lobe; CRB, cerebellum; CC, corpus callosum; IC, internal capsule; CP, cerebral peduncle; CR, corona radiata; TR, thalamic radiation; FOF, fronto-occipital fasciculus; LF, longitudinal fasciculus; FOR, forceps. Bolded values indicate statistical significance (P or P_{FDR} < 0.05). SE values are italicized. * indicates statistical significance based on the Bonferroni family-wise error corrected *P*-value threshold of 0.05/14 ROIs = 0.0035. Full results for all covariates are presented in *SI Appendix*, Tables S1 and S2.

Discussion

This cross-sectional study used MR multicomponent relaxometry to map MWF in a relatively large cohort of cognitively unimpaired adults across a broad age spectrum, revealing that higher VO_2max is associated with greater cerebral myelination. While CRF is an indication of current health, reflecting an individual's aerobic fitness level at the time of measurement, it is also influenced by cumulative lifetime physical activity and overall health. Our findings suggest that higher CRF is associated with better myelin integrity, especially at middle and older ages, which may reflect a lifelong history of physical activity and overall health. However, our study cannot establish a causal link between improved CRF and improved myelin integrity. Nevertheless, our findings suggest that CRF is likely to be a valuable indicator of overall health and a potential target for interventions aimed at promoting brain health. Future studies can build on this foundation to explore the complex relationships between physical fitness, brain health, and myelin integrity, ultimately informing strategies to support healthy brain aging and prevent neurological disorders.

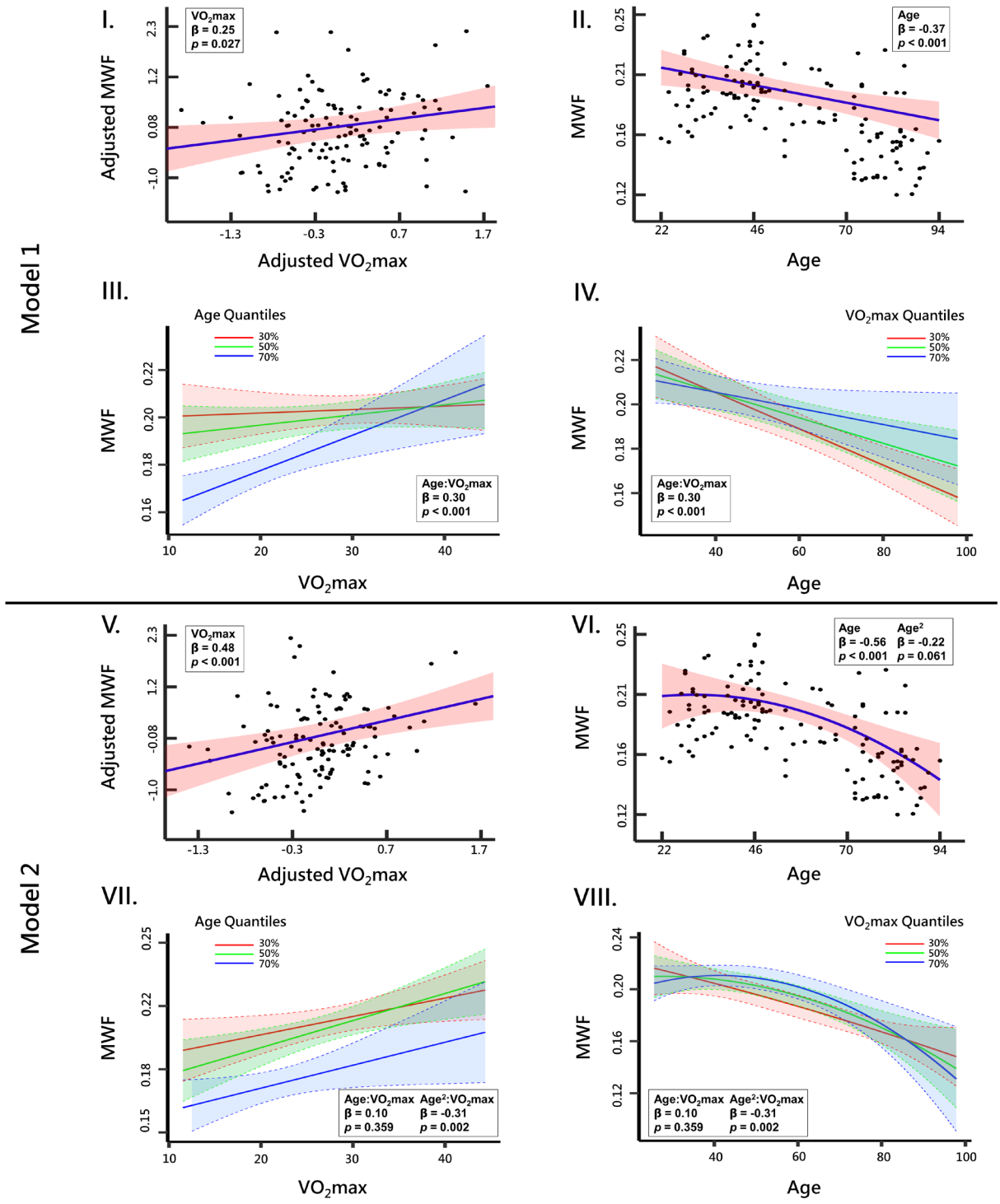

Fig. 2. Association of MWF with maximum rate of oxygen consumption (VO_2max) within the WB ROI derived using (*I*) model #1 or (*V*) model #2. The line of best fit (blue solid line), confidence bounds (shaded red region), regression coefficient (SE), and *P* value were derived from the linear regression models adjusted for covariates. The adjusted response function describes the relationship between the fitted response and MWF, with the remaining z-scored predictors set to 0. *III* and *IV* illustrate age-stratified and VO_2max-stratified associations between MWF and either standardized VO_2max or age, respectively, derived using model #1, while *VII* and *VIII* illustrate age-stratified and VO_2max-stratified associations between MWF and either standardized VO_2max or age, respectively, derived using model #2. The colored lines correspond to the 30th (red), 50th (green), and 70th (blue) quantiles of age or VO_2max. Finally, the association between age and MWF derived using model #1 or model #2 are shown in *II* and *VI*, respectively.

We found significant positive correlations between VO_2max and MWF in the frontal lobes and white matter tracts, including the internal capsule and corona radiata, supporting and extending previous findings (10, 28). Aerobic physical activity has been shown to increase brain volume and reduce cortical atrophy in vulnerable regions, including the frontal lobes. Aerobic exercise and cardiovascular fitness are known to preserve and enhance cognitive functions like working memory, task-switching, and executive function in aging humans (29), which are known to be subserved by the frontal lobes. This suggests that higher CRF may protect these regions known to be vulnerable to age-related neurodegeneration, including myelin degeneration. The internal capsule and corona radiata form a critical white matter tract involved in motor function, attention, and executive functions (30). They are vulnerable to changes in

cerebral blood flow and hypoperfusion (31), making them prone to infarctions (32). Higher CRF may protect these regions by improving blood flow, strengthening vasculature, and reducing vascular-related damage, thereby enhancing myelin integrity.

The interpretation of VO_2max is dependent on age and gender. For example, a value of 30 indicates an excellent CRF for a female above 60 y of age, while the same value indicates poor CRF for a male below the age of 30 y. To account for the possibility that VO_2max may have different associations with MWF based on age, we included an age × VO_2max interaction term in our models (and age^2 × VO_2max interaction in model #2). This interaction term allowed us the examine the MWF and VO2max associations by age. Our results suggest that the association between VO_2max and MWF is indeed modified by age, as illustrated using a separate trajectory per age quantile in Fig. 2, panels *III* and *VII*. Our finding of a strong and statistically significant age × VO_2max and age^2 × VO_2max interactions across most ROIs support the age-dependent hypothesis, with the age × VO_2max interaction term revealing a steeper decline in MWF with age in the group with lower VO_2max, while the age^2 × VO_2max interaction term indicating the nonlinear pattern of myelin maturation and decline is VO_2max-dependent with the higher VO_2max group reaching the MWF peak at later ages as compared to the other groups as indicative of improved myelination with higher CRF levels. These results suggest that a healthy lifestyle's neuroprotective effects become increasingly crucial with age as neurocognitive decline and neurodegenerative processes accelerate (33). Previous studies have shown that CRF is more strongly linked to white matter microstructure in older adults than younger adults (6, 34) and has differential effects on gray matter volume and cortical thickness between age groups (10, 35), particularly in prefrontal and temporal brain regions, consistent with findings that aerobic exercise provides greater cognitive benefits to older adults (36). Our study adds to the evidence that the relationship between CRF and brain health, specifically myelin integrity, becomes increasingly important with age, and that interventions targeting CRF improvement are crucial for preserving white matter integrity in late life. However, while our cohort spanned a wide age range, it does not include very young participants (<22 y old); this limitation derives from the exclusion criteria of the Baltimore Longitudinal Study of Aging (BLSA) and Genetic and Epigenetic Signatures of Translational Aging Laboratory Testing (GESTALT) studies which precluded a detailed characterization of the nonlinear interaction of VO_2max and age, calling for further investigations. We also note that it was not feasible to obtain optimal uniform sampling across all age intervals in this current sample of BLSA and GESTALT study participants, with the number of subjects aged 50 to 70 y being lower as compared to the other age decades. Therefore, results derived from model #2 must be interpreted with caution. To account for sex effects, our models included a main effect of sex, which adjusts for level differences in MWF. However, given our limited sample size, we were unable to investigate whether sex modifies the relationship between MWF and VO_2max and whether such sex effects may be age-dependent. Future analyses using larger cohorts will be important for further examining the age- and sex-dependent associations of VO_2max with MWF.

Research has shed light on the physiological and neurobiological mechanisms by which CRF preserves neural integrity, across both animal and human studies. Notably, aerobic exercise has been found to trigger neuroprotective adaptations in brain mitochondrial machinery, which declines with aging and is implicated in neurodegenerative diseases like Alzheimer's disease and Parkinson's disease (37). These beneficial adaptations include increased mitochondrial biogenesis, function, and energy utilization (38), upregulation of genes and proteins associated with glycolytic and oxidative neurometabolism (39), improved antioxidant capacity, and, consequently, attenuation of reactive oxygen species overproduction and oxidative stress-associated damage to cerebral tissues (37, 40). Relatedly, aerobic exercise is believed to upregulate the expression and release of key neurotrophins and growth factors, notably brain-derived neurotrophic factor (BDNF) (41), which has been shown to increase brain mitochondrial function (42), and alter mitochondrial oxidative efficiency and apoptotic signaling characteristic of neurodegenerative pathologies (37). Along with BDNF, aerobic exercise has also been shown to elevate levels of insulin-like growth factor and vascular endothelial growth factor, which are collectively believed to enhance synaptic and glial plasticity, axonal pruning, dendritic branching, neurogenesis, and angiogenesis (43–45). Moreover, physical activity has been shown to improve white matter integrity by mediating changes in cerebrovascular supply factors related to CRF, increasing proliferation of brain endothelial cells, and, therefore, optimizing oxygen and glucose delivery to cerebral tissues (46). Animal studies have further demonstrated that physical activity reduces levels of amyloid-beta (47), a neuropathological marker of AD, and proinflammatory cytokines associated with impaired white matter integrity (43). Aerobic exercise has also been shown to enhance axonal and myelin sheath regeneration and to modulate concentrations of myelination-related proteins (45). As such, by providing an in vivo assessment of the beneficial effects of CRF on myelin integrity, the results of our MWF imaging study contribute to a more in-depth demonstration of the intricate relationship between CRF and white matter microstructural integrity in humans, shedding further insight into the potential mechanisms that promote brain health and mitigate neurodegeneration throughout the aging process.

Although our investigation examined a relatively large cohort and used advanced MRI methodology to probe myelin content, our work has certain limitations. The cross-sectional nature of our study precludes the ability to establish a causal relationship between CRF and myelin content. Although our study demonstrated an age-dependent effect of VO_2max on MWF, future prospective longitudinal studies are needed to explore this relationship more comprehensively. Moreover, future interventional studies are also needed to determine the neuroprotective effects of increasing CRF more specifically on myelination in humans; this work is currently in progress. Further, while the BLSA and GESTALT participants included in this study were healthy without a history of chronic diseases, other covariates that are not accounted for here may affect determination of our results, including genetic and metabolic factors. In addition, our cohort was predominantly composed of White participants, so our results may not be generalizable to diverse populations, and future studies should aim to recruit more representative samples to enhance external validity and better address health disparities. Moreover, further evidence of the relationship between VO_2max and MWF as derived using other MWF imaging techniques is necessary. Indeed, MWF can be quantified using various MRI methods, including the well-established multi-spin-echo sequences like Car-Purcell-Meiboom-Gill (CPMG) and Gradient-and Spin-Echo (GRASE), as well as the multi-gradient-echo sequences, Look-Locker-type sequences combined with multicomponent longitudinal relaxometry analysis, and T_2-prepared module for magnetization-preparation (48). While each method has its advantages and limitations, such as availability, signal model simplicity, and susceptibility to field inhomogeneities, further developments and improvements are needed to overcome recognized limitations and provide more accurate and reliable MWF measurements. As an example, mcDESPOT derived MWF values exhibit higher values as compared to those derived from a CPMG analysis (49). This can be attributed to the fact that MRI pulse sequences, including mcDESPOT and CPMG, are influenced to substantially different degrees by experimental and physiological effects. Therefore, received signals will

deviate from their ideal models due to diffusion, exchange, off-resonance effects, magnetization transfer, *J*-coupling, spin locking, internal gradients, and magnetization spoiling. The importance of these effects will depend both upon the specifics of the sample or subject under investigation and on the details of the pulse sequence, including the selection of parameters such as echo time (TE), repetition time (TR), flip angles (FAs), and radio-frequency (RF) pulse shape, and gradient durations and amplitudes. Finally, since MWF is a fraction of total water in the voxel, increases in extracellular or intracellular water due to axonal degeneration, inflammation, or other factors could lead to artificially decreased MWF values. Further research to better understand the relationship between MWF, myelination, and water compartment changes is still needed.

Conclusion

This original study provides compelling evidence of the crucial role of CRF in the preservation of myelin integrity with advancing age, expanding our understanding of the intricate relationship between cardiovascular health and white matter microstructure. Additionally, this work lays the foundation for further investigations into the potential therapeutic applications of improving CRF or myelination to promote healthy brain aging and combat age-related neurodegeneration, including in AD.

Materials and Methods

Study Cohort. Participants were drawn from two ongoing aging cohorts at the National Institute on Aging (NIA), namely, the BLSA and the GESTALT study. The goal of the BLSA and GESTALT studies is to evaluate multiple biomarkers related to aging. We note that the inclusion and exclusion criteria for these two studies are essentially identical. Participants underwent testing at the NIA's clinical research unit and were excluded if they had metallic implants or major neurologic or medical disorders. The MRI protocol was approved by the MedStar Research Institute and the NIH Intramural Ethics Committees, and all procedures approved by the National Institutes on Aging Institutional Review Board (Protocol Number: 03-AG-0325). Informed consent was obtained from all participants.

Data Acquisition. Each participant underwent our BMC-mcDESPOT protocol for MWF mapping (21). This imaging protocol consists of 3D spoiled gradient recalled echo (SPGR) images acquired with FAs of [2 4 6 8 10 12 14 16 18 20]°, TE of 1.37 ms, TR of 5 ms, and acquisition time of ~5 min, as well as 3D balanced steady-state free precession (bSSFP) images acquired with FAs of [2 4 7 11 16 24 32 40 50 60]°, TE of 2.8 ms, TR of 5.8 ms, and acquisition time of ~6 min. The bSSFP images were acquired with RF excitation pulse phase increments of 0 or 180° to account for the off-resonance effects, with a total scan time of ~12 min. All SPGR and bSSFP images were acquired with an acquisition matrix of 150 × 130 × 94, voxel size 1.6 mm × 1.6 mm × 1.6 mm. To correct for excitation RF inhomogeneity (50), we used the double-angle method (DAM), which consisted of acquiring two fast spin-echo images with FAs of 45° and 90°, TE of 102 ms, TR of 3,000 ms, acquisition voxel size of 2.6 mm × 2.6 mm × 4 mm, and acquisition time of ~4 min. All images were acquired with field-of-view of 240 mm × 208 mm × 150 mm, SENSE factor of 2, and reconstructed to a voxel size of 1 mm × 1 mm × 1 mm. The total acquisition time was ~21 min (26). MRI scans were performed on a 3 T whole body Philips MRI system (Achieva, Best, The Netherlands) using the internal quadrature body coil for transmission and an eight-channel phased-array head coil for reception. We emphasize that all MRI studies and ancillary measurements were performed with the same MRI system, with the same pulse sequences, using the same software and hardware versions, and at the same facility for both BLSA and GESTALT participants.

Data Processing. For each participant, using the FLIRT analysis as implemented in FSL software, all SPGR, bSSFP, or DAM images were linearly registered to the SPGR image obtained at FA of 8° and the respective derived transformation matrices were then applied to the original SPGR, bSSFP, or DAM images. A whole-brain MWF map was then generated using BMC-mcDESPOT from these coregistered SPGR, bSSFP, and DAM datasets (21, 26). BMC-mcDESPOT assumes a two-relaxation time component system consisting of a short T_2 component, attributed to myelin water, and a long T_2 component, attributed to intra- and extracellular waters. We used the signal model explicitly accounting for nonzero TE (51). This emerging method offers rapid and reliable WB MWF maps within feasible clinical time (20, 21).

Further, using FSL software, the averaged SPGR image over FAs underwent nonlinear registration to the Montreal Neurological Institute (MNI) standard space, and the computed transformation matrix was then applied to the corresponding MWF maps (26). Fourteen white matter (WM) ROIs were defined from the MNI structural atlas. These encompassed the whole-brain (WB), the frontal (FL), parietal (PL), temporal (TL), and occipital (OL) lobes, cerebellum (CRB), the corpus callosum (CC), internal capsule (IC), cerebral peduncle (CP), corona radiata (CR), thalamic radiation (TR), fronto-occipital fasciculus (FOF), longitudinal fasciculus (LF), and forceps major and minor (FOR). ROIs were defined in the MNI space and have been eroded to reduce partial volume effects and imperfect image registration using a kernel box of 2 voxels × 2 voxels × 2 voxels with the FSL tool *fslmaths*. Within each ROI, the mean MWF was calculated.

CRF Measurement. CRF was assessed from a graded maximal treadmill test as per our established fitness protocol (52). Oxygen consumption was monitored continuously during a modified Balke treadmill test. The treadmill's speed was held constant (about 3.5 miles/h), and the grade of the treadmill was progressively increased by 3% at 2-min intervals until voluntary exhaustion. In subjects with higher fitness, treadmill speed was increased by 0.5 miles/h 1 to 3 times during the test to achieve exhaustion. Expired gas volumes were measured using either Tissot tanks or a Parkinson-Cowan gas meter (Waitsfield, Virginia). Expired oxygen and carbon dioxide concentrations were measured using either dedicated oxygen and carbon dioxide analyzers or a medical mass spectrometer (Perkin-Elmer MGA-1110, Milwaukee, Wisconsin). Oxygen consumption was calculated every 30 s, and the highest value was termed VO_2max, expressed in milliliters per kilogram body weight per minute (mL/kg/min).

Statistical Analysis. Multiple linear regression analyses were used to investigate the correlation of VO_2max with MWF. The average MWF value within each ROI was considered as the dependent variable. In our first analysis (model #1), age, VO_2max, sex, and SBP were considered as independent variables. A continuous age × VO_2max interaction term was also included as an independent variable to assess whether association between VO_2max on MWF was significantly different according to age. Studies have shown that MWF follows a quadratic association with age. Therefore, we conducted a second analysis (model #2) incorporating age^2 and age^2 × VO_2max as additional covariates. In all analyses, the continuous dependent and independent variables were Z-scored by subtracting the mean value calculated across participants from each measured value and dividing by the SD value. The threshold for statistical significance was defined as $P < 0.05$. *P*-values are shown with and without the FDR correction to allow readers to consider the trade-off between Type I and Type II errors and make informed decisions about the significance of our findings. All analyses were run using MATLAB or R software.

Data, Materials, and Software Availability. All source data and codes used for creating the main manuscript figures and tables are available at: https://github.com/mrpadunit/cardiorespiratory_vs_myelin (53). MRI images will be available under permissioned data access, in accordance with NIA policy (https://blsa.nih.gov/faq) (54). Deidentified data are accessible to investigators and collaborators. To access permissioned data, investigators can apply online through the BLSA Data Use page as described in https://blsa.nih.gov/faq (54). Additional requirements, such as Data and Material Transfer Agreements, may apply for external investigators (https://blsa.nih.gov/faq) (54).

ACKNOWLEDGMENTS. This work was supported by the National Institute of Aging of the NIH Intramural Research Program. This work utilized the computational resources of the NIH HPC Biowulf cluster (https://hpc.nih.gov).

Author affiliations: [a]Laboratory of Clinical Investigation, National Institute on Aging, NIH, Baltimore, MD 21224; [b]Laboratory of Behavioral Neuroscience, National Institute on Aging, NIH, Baltimore, MD 21224; [c]Translational Gerontology Branch, National Institute on Aging, NIH, Baltimore, MD 21224; and [d]Clinical Research Core, National Institute on Aging, NIH, Baltimore, MD 21224

Author contributions: L.F., and M. Bouhrara designed research; C.M.B., J. Bergeron, and M. Bouhrara acquired the MRI data; M.E.F., Z.G., M. Bilgel, L.F., and M. Bouhrara performed research; M.E.F., Z.G., M. Bilgel, J.P.L., A.G., J. Bae, E.P., M.K., C.M.B., J. Bergeron, S.C., J.D., L.F., and M. Bouhrara contributed new reagents/analytic tools; M.E.F., Z.G., M. Bilgel, J.B., and M. Bouhrara analyzed data; M.E.F., Z.G., and M. Bouhrara wrote the paper; and M.E.F., Z.G., M. Bilgel, J.P.L., A.G., J. Bae, E.P., M.K., C.M.B., J. Bergeron, L.F., and M. Bouhrara edited the paper.

1. S. Lee *et al.*, White matter hyperintensities are a core feature of Alzheimer's disease: Evidence from the dominantly inherited Alzheimer network. *Ann. Neurol.* **79**, 929–939 (2016).
2. A. Wu *et al.*, Association of brain magnetic resonance imaging signs with cognitive outcomes in persons with nonimpaired cognition and mild cognitive impairment. *JAMA Netw. Open* **2**, e193359 (2019).
3. F. Fazekas *et al.*, Pathologic correlates of incidental MRI white matter signal hyperintensities. *Neurology* **43**, 1683–1689 (1993).
4. K. I. Erickson, A. M. Weinstein, O. L. Lopez, Physical activity, brain plasticity, and Alzheimer's disease. *Arch. Med. Res.* **43**, 615–621 (2012).
5. S. M. Hayes, J. P. Hayes, M. Cadden, M. Verfaellie, A review of cardiorespiratory fitness-related neuroplasticity in the aging brain. *Front. Aging Neurosci.* **5**, 31 (2013).
6. S. M. Hayes, D. H. Salat, D. E. Forman, R. A. Sperling, M. Verfaellie, Cardiorespiratory fitness is associated with white matter integrity in aging. *Ann. Clin. Transl. Neurol.* **2**, 688–698 (2015).
7. C. E. Sexton *et al.*, A systematic review of MRI studies examining the relationship between physical fitness and activity and the white matter of the ageing brain. *Neuroimage* **131**, 81–90 (2016).
8. D. E. Barnes, K. Yaffe, W. A. Satariano, I. B. Tager, A longitudinal study of cardiorespiratory fitness and cognitive function in healthy older adults. *J. Am. Geriatr. Soc.* **51**, 459–465 (2003).
9. R. J. Dougherty *et al.*, Cardiorespiratory fitness mitigates brain atrophy and cognitive decline in adults at risk for Alzheimer's disease. *Alzheimers Dement. (Amst).* **13**, e12212 (2021).
10. S. J. Colcombe *et al.*, Aerobic fitness reduces brain tissue loss in aging humans. *J. Gerontol. A Biol. Sci. Med. Sci.* **58**, 176–180 (2003).
11. N. Zhu *et al.*, Cardiorespiratory fitness and brain volume and white matter integrity: The CARDIA study. *Neurology* **84**, 2347–2353 (2015).
12. N. F. Johnson, A. A. Bahrani, D. K. Powell, G. A. Jicha, B. T. Gold, Cardiorespiratory fitness diminishes the effects of age on white matter hyperintensity volume. *PLoS One* **15**, e0236986 (2020).
13. C. J. Vesperman *et al.*, Cardiorespiratory fitness attenuates age-associated aggregation of white matter hyperintensities in an at-risk cohort. *Alzheimers Res. Ther.* **10**, 97 (2018).
14. Q. Tian *et al.*, Cardiorespiratory fitness and brain diffusion tensor imaging in adults over 80 years of age. *Brain Res.* **1588**, 63–72 (2014).
15. F. T. Chen, K. I. Erickson, H. Huang, Y. K. Chang, The association between physical fitness parameters and white matter microstructure in older adults: A diffusion tensor imaging study. *Psychophysiology* **57**, e13539 (2020).
16. R. D. Perea *et al.*, Cardiorespiratory fitness and white matter integrity in Alzheimer's disease. *Brain Imaging Behav.* **10**, 660–668 (2016).
17. K. Ding *et al.*, Cardiorespiratory fitness and white matter neuronal fiber integrity in mild cognitive impairment. *J. Alzheimers Dis.* **61**, 729–739 (2018).
18. R. S. Prakash, E. M. Snook, R. W. Motl, A. F. Kramer, Aerobic fitness is associated with gray matter volume and white matter integrity in multiple sclerosis. *Brain Res.* **1341**, 41–51 (2010).
19. M. E. Faulkner *et al.*, Harnessing myelin water fraction as an imaging biomarker of human cerebral aging, neurodegenerative diseases, and risk factors influencing myelination: *A review. J Neurochem.*, 10.1111/jnc.16170 (2024).
20. M. Bouhrara *et al.*, Adult brain aging investigated using BMC-mcDESPOT-based myelin water fraction imaging. *Neurobiol. Aging* **85**, 131–139 (2020).
21. M. Bouhrara, R. G. Spencer, Rapid simultaneous high-resolution mapping of myelin water fraction and relaxation times in human brain using BMC-mcDESPOT. *Neuroimage* **147**, 800–811 (2017).
22. M. Bouhrara *et al.*, Improved determination of the myelin water fraction in human brain using magnetic resonance imaging through Bayesian analysis of mcDESPOT. *Neuroimage* **127**, 456–471 (2016).
23. M. Bouhrara *et al.*, Association of cerebral blood flow with myelin content in cognitively unimpaired adults. *BMJ Neurol. Open* **2**, e000053 (2020).
24. M. Kiely *et al.*, Evidence of An Association Between Cerebral Blood Flow and Microstructural Integrity in Normative Aging Using a Holistic MRI Approach. *J. Magn. Reson. Imaging* **58**, 284–293 (2023).
25. M. E. Faulkner *et al.*, Lower myelin content is associated with lower gait speed in cognitively unimpaired adults. *J. Gerontol. A Biol. Sci. Med. Sci.* **78**, 1339–1347 (2023).
26. J. P. Laporte *et al.*, Hypertensive adults exhibit lower myelin content: A multicomponent relaxometry and diffusion magnetic resonance imaging study. *Hypertension* **80**, 1728–1738 (2023), 10.1161/hypertensionaha.123.21012.
27. M. Bouhrara *et al.*, Evidence of association between obesity and lower cerebral myelin content in cognitively unimpaired adults. *Int. J. Obesity* **45**, 850–859 (2021).
28. K. I. Erickson *et al.*, Exercise training increases size of hippocampus and improves memory. *Proc. Natl. Acad. Sci. U.S.A.* **108**, 3017–3022 (2011).
29. S. J. Colcombe *et al.*, Aerobic exercise training increases brain volume in aging humans. *J. Gerontol. A Biol. Sci. Med. Sci.* **61**, 1166–1170 (2006).
30. I. S. Buyanova, M. Arsalidou, Cerebral white matter myelination and relations to age, gender, and cognition: A selective review. *Front. Hum. Neurosci.* **15**, 662031 (2021).
31. D. M. Moody, M. A. Bell, V. R. Challa, Features of the cerebral vascular pattern that predict vulnerability to perfusion or oxygenation deficiency: An anatomic study. *AJNR Am. J. Neuroradiol.* **11**, 431–439 (1990).
32. T. Koyama *et al.*, Diffusion tensor imaging for intracerebral hemorrhage outcome prediction: Comparison using data from the corona radiata/internal capsule and the cerebral peduncle. *J. Stroke Cerebrovasc. Dis.* **22**, 72–79 (2013).
33. K. Hotting, B. Roder, Beneficial effects of physical exercise on neuroplasticity and cognition. *Neurosci. Biobehav. Rev.* **37**, 2243–2257 (2013).
34. R. A. Mace, D. A. Gansler, K. S. Sawyer, M. Suvak, Age-dependent relationship of cardiorespiratory fitness and white matter integrity. *Neurobiol. Aging* **105**, 48–56 (2021).
35. V. J. Williams *et al.*, Cardiorespiratory fitness is differentially associated with cortical thickness in young and older adults. *Neuroimage* **146**, 1084–1092 (2017).
36. S. Colcombe, A. F. Kramer, Fitness effects on the cognitive function of older adults: A meta-analytic study. *Psychol. Sci.* **14**, 125–130 (2003).
37. I. Marques-Aleixo, P. J. Oliveira, P. I. Moreira, J. Magalhaes, A. Ascensao, Physical exercise as a possible strategy for brain protection: Evidence from mitochondrial-mediated mechanisms. *Prog. Neurobiol.* **99**, 149–162 (2012).
38. J. L. Steiner, E. A. Murphy, J. L. McClellan, M. D. Carmichael, J. M. Davis, Exercise training increases mitochondrial biogenesis in the brain. *J. Appl. Physiol.* **111**, 1066–1071 (2011).
39. Q. Ding, S. Vaynman, P. Souda, J. P. Whitelegge, F. Gomez-Pinilla, Exercise affects energy metabolism and neural plasticity-related proteins in the hippocampus as revealed by proteomic analysis. *Eur. J. Neurosci.* **24**, 1265–1276 (2006).
40. A. Navarro, C. Gomez, J. M. Lopez-Cepero, A. Boveris, Beneficial effects of moderate exercise on mice aging: Survival, behavior, oxidative stress, and mitochondrial electron transfer. *Am. J. Physiol. Regul. Integr. Comp. Physiol.* **286**, R505–R511 (2004).
41. P. A. Adlard, V. M. Perreau, C. W. Cotman, The exercise-induced expression of BDNF within the hippocampus varies across life-span. *Neurobiol. Aging* **26**, 511–520 (2005).
42. A. Markham, I. Cameron, P. Franklin, M. Spedding, BDNF increases rat brain mitochondrial respiratory coupling at complex I, but not complex II. *Eur. J. Neurosci.* **20**, 1189–1196 (2004).
43. C. W. Cotman, N. C. Berchtold, Exercise: A behavioral intervention to enhance brain health and plasticity. *Trends Neurosci.* **25**, 295–301 (2002).
44. M. J. Kujawa *et al.*, Physical activity and the brain myelin content in humans. *Front. Cell Neurosci.* **17**, 1198657 (2023).
45. A. L. Graciani, M. U. Gutierre, A. A. Coppi, R. M. Arida, R. C. Gutierre, Myelin, aging, and physical exercise. *Neurobiol. Aging* **127**, 70–81 (2023).
46. A. Z. Burzynska *et al.*, Physical activity and cardiorespiratory fitness are beneficial for white matter in low-fit older adults. *PLoS One* **9**, e107413 (2014).
47. P. A. Adlard, V. M. Perreau, V. Pop, C. W. Cotman, Voluntary exercise decreases amyloid load in a transgenic model of Alzheimer's disease. *J. Neurosci.* **25**, 4217–4221 (2005).
48. G. F. Piredda, T. Hilbert, J.-P. Thiran, T. Kober, Probing myelin content of the human brain with MRI: A review. *Magn. Reson. Med.* **85**, 627–652 (2021).
49. J. Zhang, S. H. Kolind, C. Laule, A. L. MacKay, Comparison of myelin water fraction from multiecho T2 decay curve and steady-state methods. *Magn. Reson. Med.* **73**, 223–232 (2015).
50. M. Bouhrara, R. G. Spencer, Steady-state double-angle method for rapid B(1) mapping. *Magn. Reson. Med.* **82**, 189–201 (2019).
51. M. Bouhrara, R. G. Spencer, Incorporation of nonzero echo times in the SPGR and bSSFP signal models used in mcDESPOT. *Magn. Reson. Med.* **74**, 1227–1235 (2015).
52. L. A. Talbot, E. J. Metter, J. L. Fleg, Leisure-time physical activities and their relationship to cardiorespiratory fitness in healthy men and women 18–95 years old. *Med. Sci. Sports Exerc.* **32**, 417–425 (2000).
53. M. E. Faulkner *et al.*, Cardiorespiratory fitness and myelin. GitHub. https://github.com/mrpadunit/cardiorespiratory_vs_myelin. Deposited 1 July 2024.
54. National Institute on Aging, Baltimore Longitudinal Study of Aging. National Institute on Aging. https://blsa.nih.gov/faq. Deposited 1 February 2022.